Electronic supplementary information for Optical characterization of DNA origami-shaped silver nanoparticles created through biotemplated lithography

Kabusure M. Kabusure[1], Petteri Piskunen[2], Jiaqi Yang[1], Mikko Kataja[1], Mwita Chacha[1], Sofia Ojasalo[2], Boxuan Shen[2,3], Tommi K. Hakala[1,*] & Veikko Linko[2,4,*]

[1]Department of Physics and Mathematics, University of Eastern Finland, Yliopistokatu 2, P.O Box 111, FI-80101, Joensuu, Finland

[2]Biohybrid Materials, Department of Bioproducts and Biosystems, Aalto University, P.O. Box 16100, 00076 Aalto, Finland

[3]Department of Medical Biochemistry and Biophysics, Karolinska Institutet, 17165 Stockholm, Sweden

[4]LIBER Centre, Aalto University, P.O. Box 16100 FI-00076, Aalto, Finland

[*]Correspondence and requests for materials should be addressed to tommi.hakala@uef.fi or veikko.linko@aalto.fi

Supplementary methods

AFM images of DNA origami templates

Atomic force microscopy (AFM) was used to verify the integrity of the biotemplates employed in BLIN (DNA origami bowties [S1] and Rothemund triangles [S2]). The templates were first immobilized on an imaging substrate by depositing 10 μl of 0.4 nM DNA origami solution in folding buffer (composed of 1$\times$ TAE buffer (40 mM Tris, 19 mM acetic acid, 1 mM ethylenediaminetetraacetic acid (EDTA)) with 12.5 mM Mg^{2+} at pH $\sim$8.3) on freshly cleaved mica chips. The chips were then incubated for 5 minutes at room temperature, followed by rinsing with 100 μl of ddH_2O. The rinse was repeated 3 times and the chips were subsequently dried with a N_2 flow. The chips were then imaged with a Bruker Dimension Icon AFM using the ScanAsyst Air imaging mode and ScanAsyst Air tips.

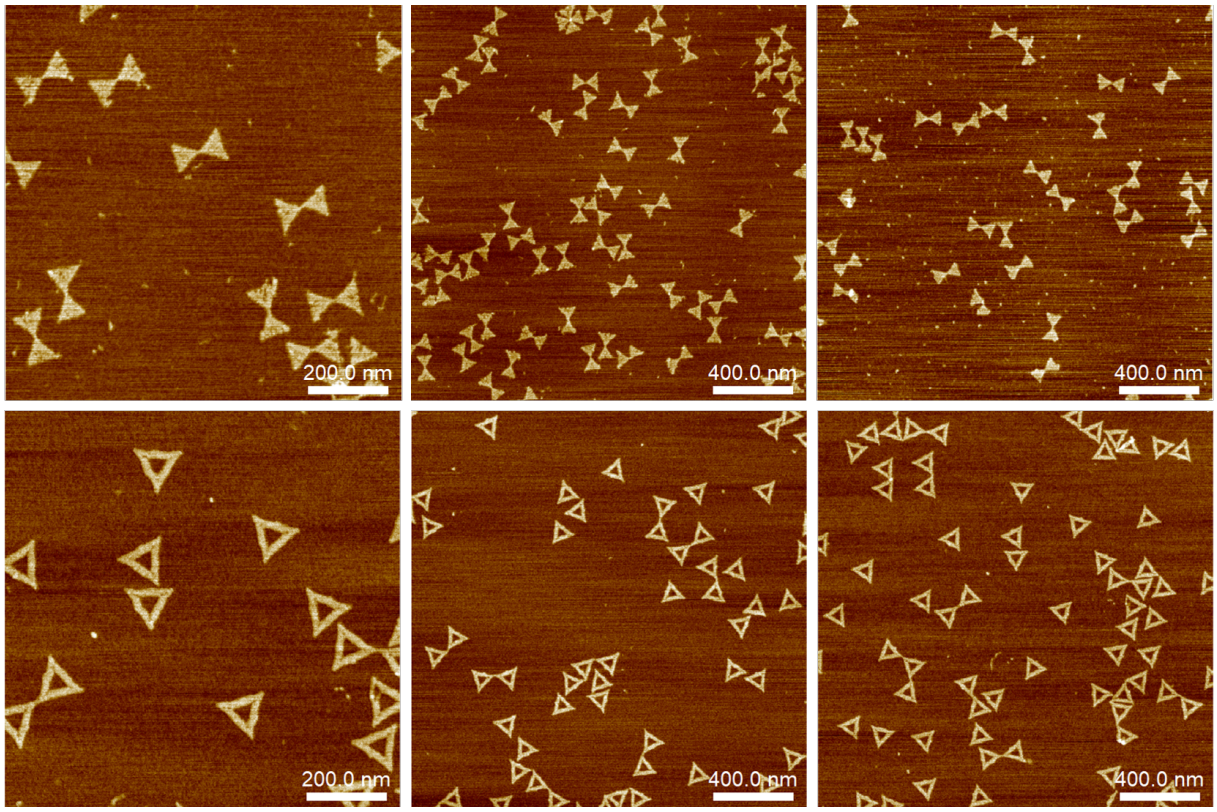

Supplementary Figure S 1. AFM images of used DNA origami templates on mica. Top panel: Bowties. Bottom panel: Rothemund triangles.

Large-scale SEM images and particle coverage of patterned chips

To determine the scales of relative surface areas and particle counts for the fabricated structures, scanning electron micrsocope (SEM) images of the measured samples were analyzed using ImageJ/Fiji [S3]. The images were turned into black and white binary images using thresholding. The binary images were then denoised with the despecle and minimum filter-functions (minimum filter at 0.1 pixels) and subsequently manually cleared to include only target particles (isolated bowties and triangles). Finally, the build in *Particle Analysis* tool was employed to determine particle surface areas and counts in relation to the total image surface area. The bowties covered between 0.5–1.2% of the ITO glass surface. Correspondingly, the triangles covered between 0.5–1.5% of the sample surface. All SEM images before and after processing are given below.

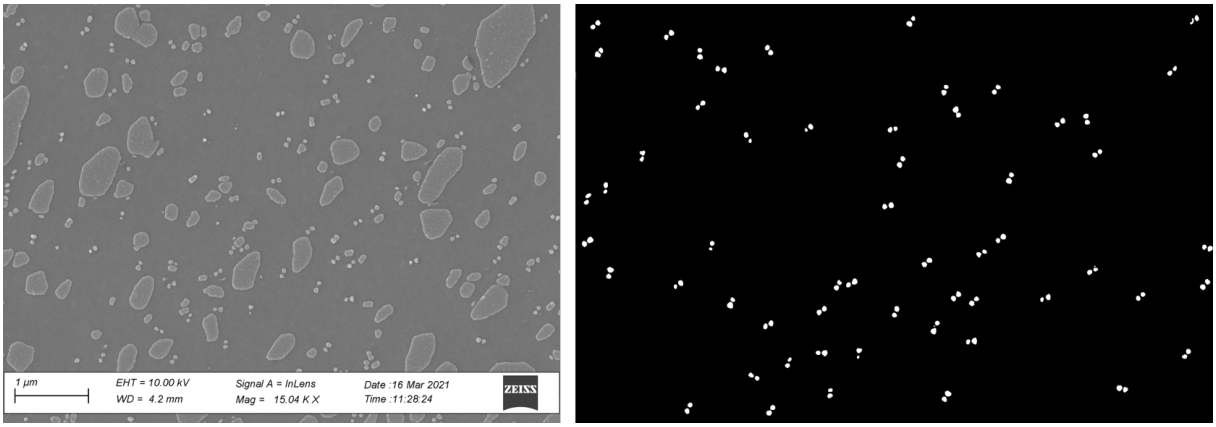

Supplementary Figure S 2. Left panel: Unprocessed SEM image input. Right panel: processed binary image used for determining bowtie particle coverage.

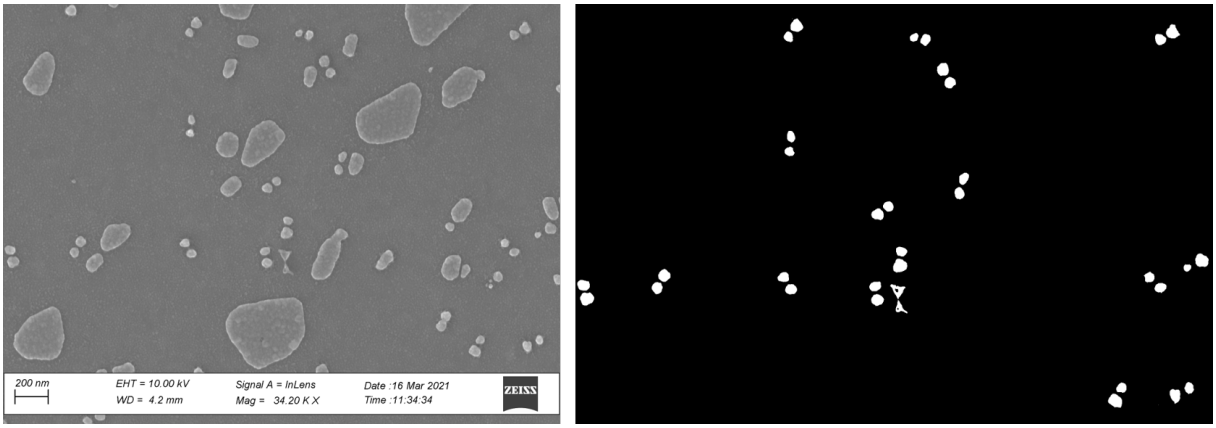

Supplementary Figure S 3. Left panel: Unprocessed SEM image input. Right panel: processed binary image used for determining bowtie particle coverage.

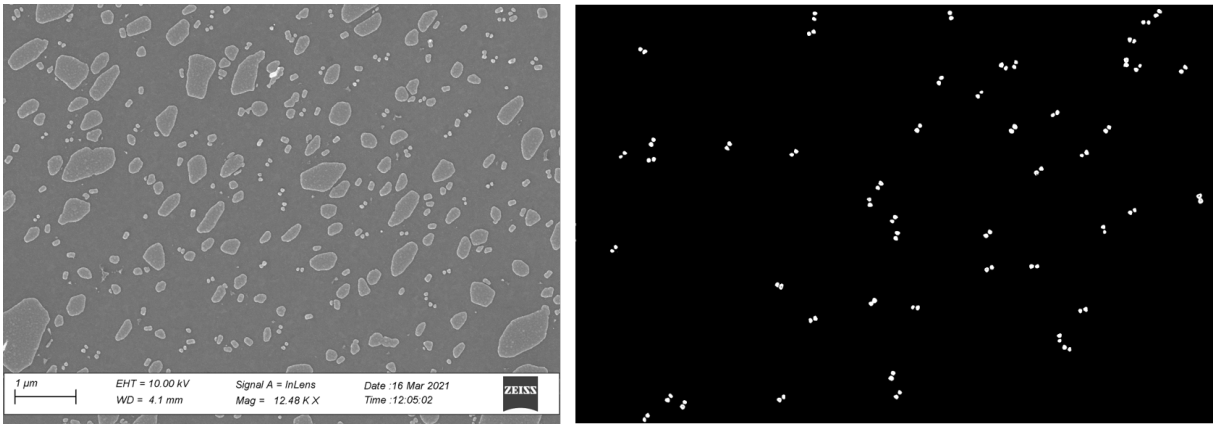

Supplementary Figure S 4. Left panel: Unprocessed SEM image input. Right panel: processed binary image used for determining bowtie particle coverage.

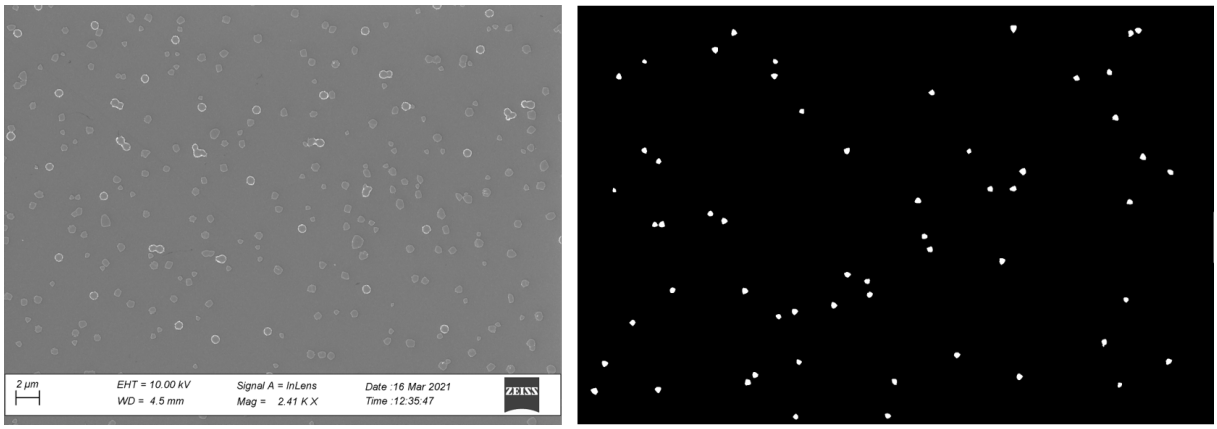

Supplementary Figure S 5. Left panel: Unprocessed SEM image input. Right panel: processed binary image used for determining single triangle particle coverage.

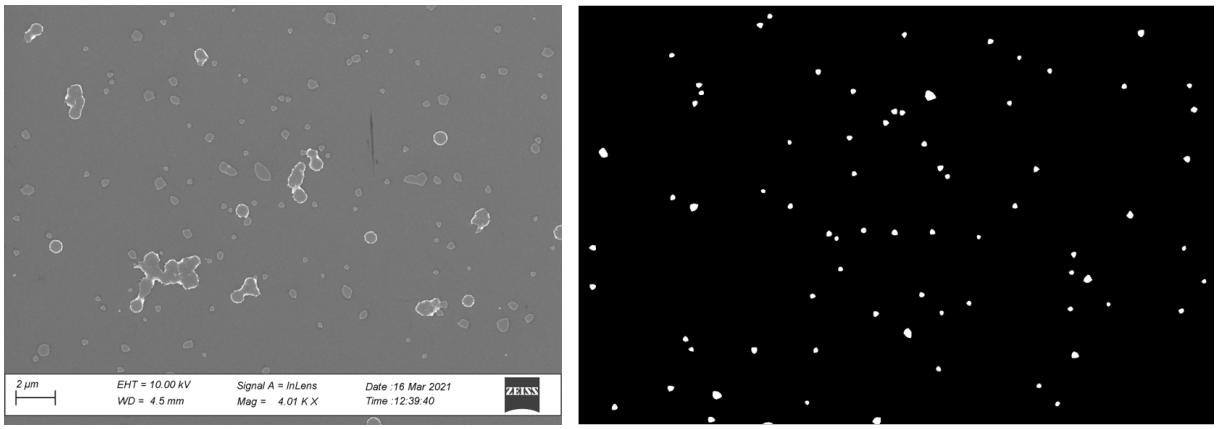

Supplementary Figure S 6. Left panel: Unprocessed SEM image input. Right panel: processed binary image used for determining single triangle particle coverage.

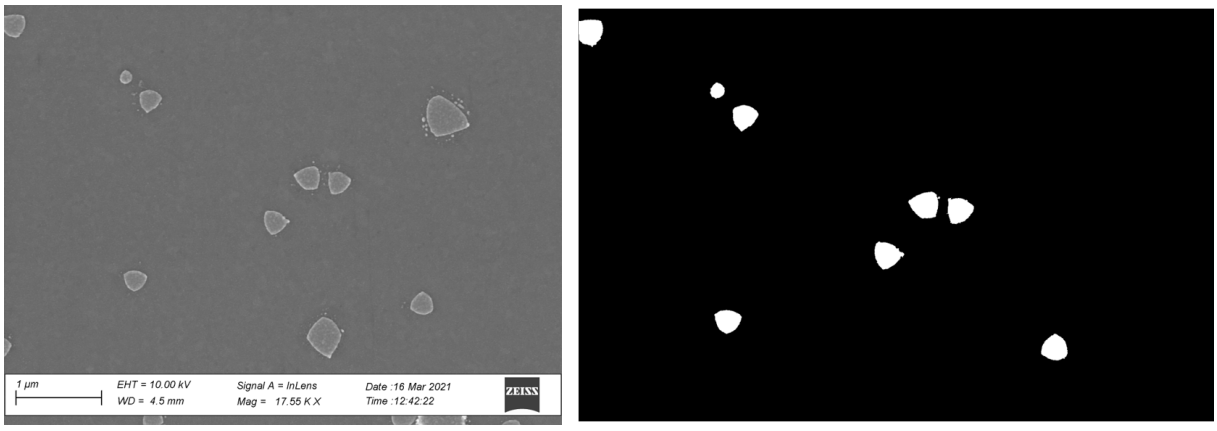

Supplementary Figure S 7. Left panel: Unprocessed SEM image input. Right panel: processed binary image used for determining single triangle particle coverage.

Simulated absorption and scattering cross-section for an individual single triangle

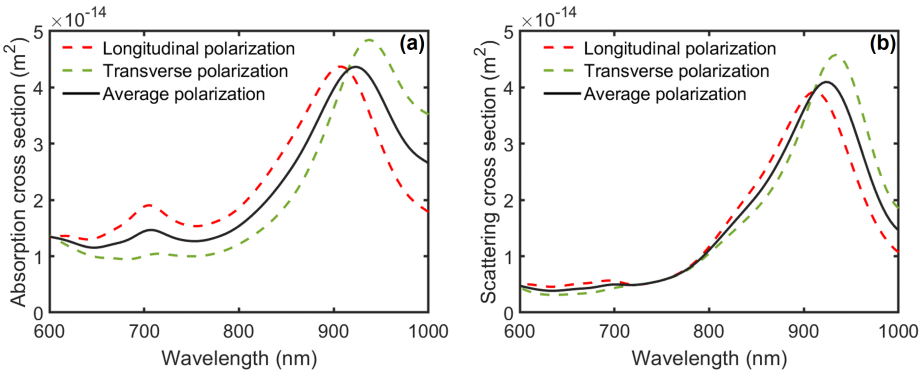

Supplementary Figure S 8. Simulations of the absorption (a) and scattering (b) cross-sections (m^2) of the single triangle vs. wavelength.

Simulated absorption and scattering cross-section for an individual bowtie

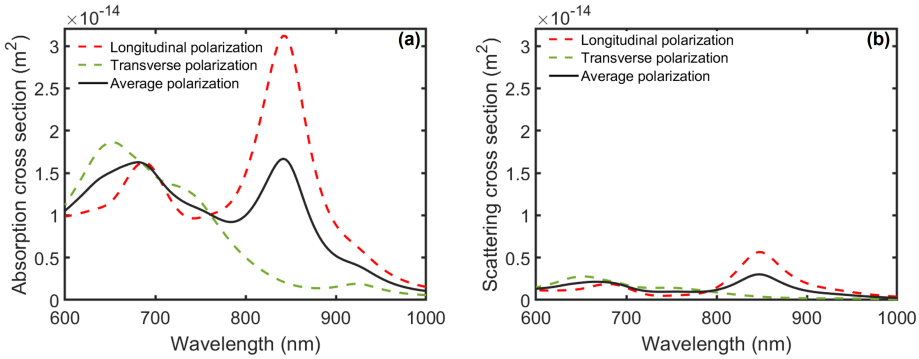

Supplementary Figure S 9. Simulations of the absorption (a) and scattering (b) cross-sections (m^2) of the bowtie vs. wavelength.

Supplementary information references

[S1] B. Shen, V. Linko, K. Tapio, S. Pikker, T. Lemma, A. Gopinath, K. V. Gothelf, M. A. Kostiainen and J. J. Toppari, *Sci. Adv.*, 2018, **4**, eaap8978.

[S2] P. W. K. Rothemund, *Nature*, 2006, **440**, 297–302.

[S3] J. Schindelin, I. Arganda-Carreras, E. Frise, V. Kaynig, M. Longair, T. Pietzsch, S. Preibisch, C. Rueden, S. Saalfeld, B. Schmid, J-Y. Tinevez, D. J. White, V. Hartenstein, K. Eliceiri, P. Tomancak and A. Cardona, *Nat. Methods*, 2012, **9**, 676–682.